SUPPLEMENT

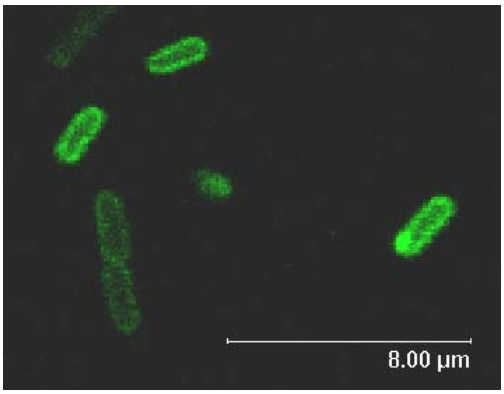

Figure S1. Confocal image of living *E. coli* with EGFP-a-F_oF_1 (pulsed excitation at 488 nm, PicoTA490). The F_oF_1-ATP synthases are located at the bacterial membrane.

Microscope setup for FRET-labeled F_oF_1-ATP synthase with a-EGFP-γ106-Alexa568

In addition to the single-molecule FRET experiments with the FRET acceptor fluorophore bound to the ε subunit, double-labeled F_oF_1-ATP synthase with the FRET acceptor Alexa568 bound to residue 106 of the γ subunit was studied using a different confocal microscope setup. The 476 nm laser line of a krypton ion laser (continuous wave, attenuated to 150 µW) excited a nearly diffraction limited volume in the buffered proteoliposome solution. Scattered laser light was blocked by a dichrioc beam splitter in epi-fluorescence configuration (DELP485, AHF, Germany). A 100 µm pinhole was used to suppress out-of-focus fluorescence. The emission of the two fluorophores was split by a second dicroic (DCXR575, AHF). Single photons were detected simultaneously by two avalanche photodiodes (SPCM-AQR-15, Perkin Elmer) after passing an interference filter HQ 516/60 for EGFP, or HQ608/60 for Alexa 568, respectively. Detection efficiencies were η_D= 0.343 for EGFP and η_A= 0.323 for Alexa568. The cross-talk of 5.8% from donor fluorescence in the acceptor channel was corrected.
The photons were counted by a multichannel scaler card (PMS 300, Becker & Hickl, Germany) with a time resolution of 1 ms. The mean diffusion time was 14 ms for proteoliposomes and 0.28 ms for rhodamine 110 as calculated from the autocorrelation functions measured with a hardware correlator (ALV5000/fast, ALV, Germany).

Preparation of FRET-labeled F_oF_1-ATP synthase with a-EGFP-γ106-Alexa568

The FRET-labeled F_oF_1-ATP synthase with γ106-Alexa568 was prepared as described for the ε56-Alexa568 labeled ATP synthase. Plasmid pRA114 with the cysteine mutant in the γ subunit was expressed in *E. coli* strain RA1 to purify the F_1 parts. The fluorophore labeling efficiency according to UV-VIS absorption spectra was 30 % for Alexa568-maleimide at γ106.

Single-molecule FRET of F_oF_1-ATP synthase with a-EGFP-γ106-Alexa568

During ATP hydrolysis in the presence of 1mM ATP, three distinct FRET levels in the FRET-efficiency trajectories (blue traces in Figure S2) indicate the 120° rotary motion of the *γ* subunit with respect to *a*. The sequence of FRET level transitions is L-M-H- as in the case of ε56 (see text). Upon ATP synthesis condition, the order of FRET level transition was reversed (Figure S2B).
The distribution of all intermediary FRET levels is shown in Figure S3 and was fitted with the gaussians. The dwell times of the three FRET levels are shown in Figure S4. Monoexponential decay fittings revealed distinct dwell times for the three γ subunit orientations.

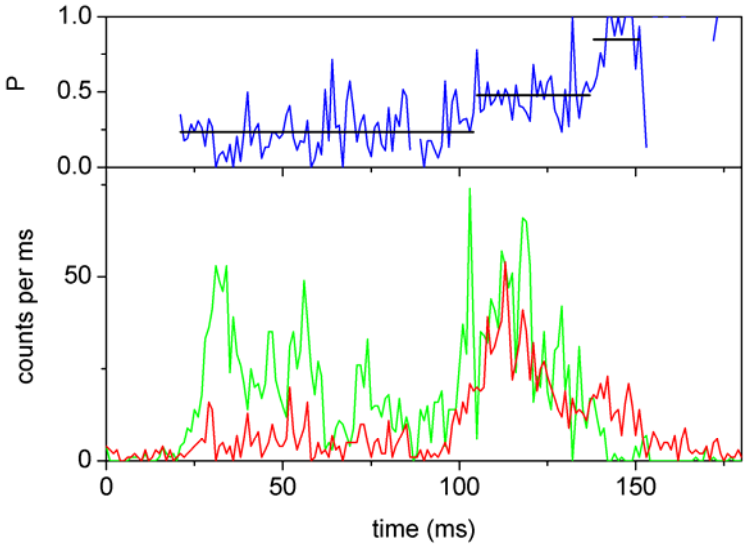

Figure S2A. Photon burst of a single FRET-labeled F_oF_1-ATP synthase with *a*-EGFP-*γ*106-Alexa568 during ATP hydrolysis. Lower panel shows fluorescence intensities of FRET donor EGFP fused to subunit *a* (green trace) and FRET acceptor Alexa568 (red trace) bound to γ106. Upper panel shows the calculated proximity factor P (blue trace) with 1 ms time resolution and the mean P value for each assigned FRET level (black line). The order of FRET level transitions is low→medium→high.

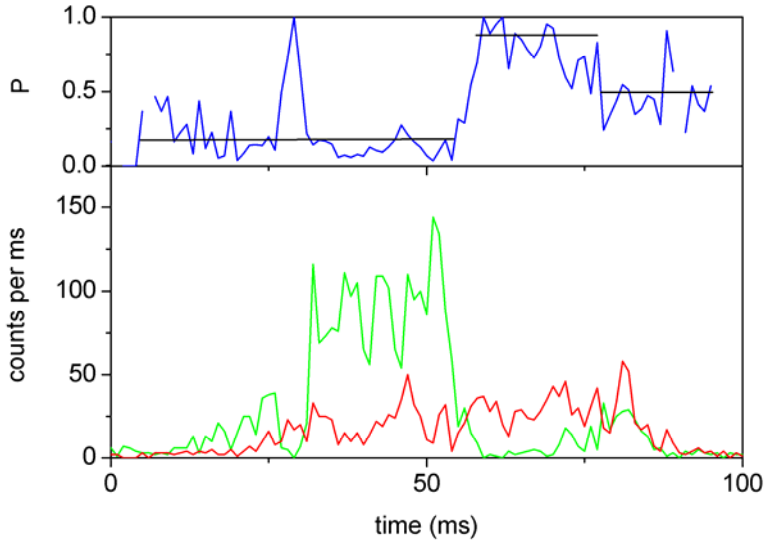

Figure S2B. Photon burst of a single FRET-labeled F_oF_1-ATP synthase with *a*-EGFP-*γ*106-Alexa568 during ATP synthesis showing the opposite order of FRET level transitions. Lower panel shows fluorescence intensities of FRET donor EGFP fused to subunit *a* (green trace) and FRET acceptor Alexa568 (red trace) bound to γ106. Upper panel shows the calculated proximity factor P (blue trace) with 1 ms time resolution and the mean P value for each assigned FRET level (black line). The order of FRET level transitions is low→high →medium.

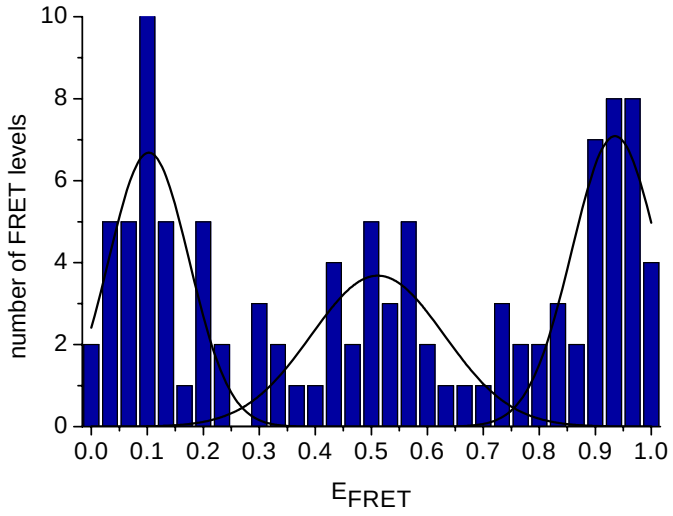

Figure S3. FRET efficiency distribution for rotating F_oF_1-ATP synthases with *a*-EGFP-γ106-Alexa568 during ATP hydrolsis. Three maxima are found at E_{FRET}= 0.1 (L level), E_{FRET}= 0.51 (M level), and E_{FRET}= 0.94 (H level).

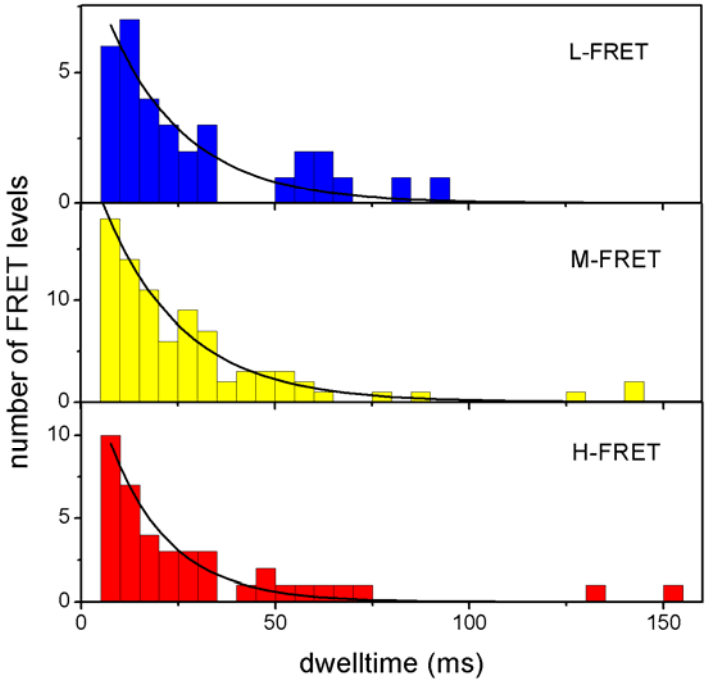

Figure S4: Dwelltime distributions during ATP hydrolysis with monoexponential decay fitting. All FRET level (19.4 ms, 159 level, data not shown), L level (20.3 ms, 34 level) in blue, M level (20.2 ms, 85 level) in yellow, H level (16.0 ms, 40 level) in red, respectively.

Errors in single-molecule FRET distance measurements

For the single-molecule FRET based distance analysis, we were concerned about the problem of excitation power dependent spectral shifts observed for single EGFP on subunit *a*. Using ps pulsed excitation, a sub-population of EGFP with red shifted fluorescence and shortened lifetimes was generated even at moderate excitation power. These spectral shifts will results in a time dependent change of the Förster radius. To measure the likelyhood and to estimate a reversibility of the spectral fluctuations, the EGFP fluorescence was split into two spectral ranges between 497 – 532 nm and 532 – 567 nm and were recorded simultaneously in an ratiometric independent single-molecule measurement. Only a small fraction (< 10 percent) of EGFP switched into a red shifted variant within a single photon burst, and most of these spontaneous spectral shifts were found to happen from the normal fluorescence to a red shifted one (M. G. Düser, unpublished). The mean brightness of the red shifted EGFP variant was lower. If this is due to less efficient excitation with 488 nm, the red shifted EGFP variant yield only a dim FRET level which is likely to be omitted by the intensity threshold filtering used for the FRET histograms.

Using the reduced fluorescence quantum yield of 0.4 for EGFP fused to subunit *a*, the Förster radius of R_0=4.9 nm for the FRET pair with Alexa568 has been determined here. Accordingly, the mean distances for the three ε56 (or γ106) orientations with respect to *a* match the distance range accessible from FRET measurements. We noticed that the single-molecule anisotropy measurements for EGFP on *a* yielded r=0.3, that is comparable but not higher than the value of the EGFP protein in solution. However, the anisotropy values for single photon bursts of Alexa568 bound to ε56 in F_oF_1-ATP synthase were smaller than 0.1. Therefore, the orientation factor κ^2 problem for calculating the FRET efficiency was neglected and κ^2=2/3 was assumed.

The width of the FRET level distributions for the three FRET efficiencies is likely to be related to the spectral fluctuations of the EGFP fluorescence. The two subensembles of EGFP were found to differ not only in their fluorescence lifetimes, but also in their relative emission spectra. Small conformational changes in the vicinity of the chromophore of EGFP might result in the distinct types of red shifted emission spectra. This would cause the photon count rates in the FRET donor channel to change, and as a consequence, the calculated FRET efficiencies would be different for equal distances. In addition, transient adhesion of the fluorophore to the surrounding protein structure could cause deviations from the assumed value for orientation factor $\kappa^2 = 2/3$.

If we assume that the EGFP would be flexible on the millisecond time scale it could result in apparent FRET changes due to changes of the distance of the EGFP chromophore with respect to the non-moving FRET acceptor. However, we would not expect a sequential order of FRET distance changes 1-2-3-1- due to wobbling (as we observed as the preferred order for 80 percent of all experimental FRET transition data), but instead would observe random FRET transitions like 1-2-1 or even 1-2-3-2-1, that is forward-backward movements. However, any photon bursts showing this kind of FRET changes were explicitly omitted from further data analysis as stated in the manuscript, so they do not contribute to the triangulation or to the dwell time analysis. In addition, the dwell time analysis clearly demonstrated the differences between the FRET acceptor on ε56 or γ106, which also contradicts EGFP wobbling.

Errors in dwell time analysis for the F_oF_1-ATP synthase with a-EGFP-ε56-Alexa568

Fitting dwell times with monoexponential decays results in slightly different numbers depending on the time intervals used for binning. For example, using 3 ms time intervals for binning we obtained dwell times of 7.8 ± 0.9 (mean±σ, standard deviation for the monoexponential fittings) ms for the L state (ε56), 10.5 ± 0.5 ms for the M state, and 8.5 ± 1.0 ms for the H state. Accordingly, the same order of dwell times was found as for the binning of 5 ms. In addition, 4 ms binning yielded similar results. Again the same order of dwell times was obtained, with the low FRET orientation of ε56 associated with the shortest dwell time. Therefore we are confident, that the distinct dwell times for ε56 are not an artifact of the 5 ms pre-binning.